frontiers in Energy Research

ORIGINAL RESEARCH
published: 18 November 2021
doi: 10.3389/fenrg.2021.793032

Roles of Oxygen Vacancies in $NiMoO_4$: A First-Principles Study

Yuanbin Wen[1,2], *Pengcheng Wang*[1,2], *Xinying Ding*[1,2], *Xiaobo Feng*[1,2] *and Chen Qing*[1,2]*

[1]*Yunnan Key Lab of Opto-Electronic Information Technology, Yunnan Normal University, Kunming, China,* [2]*College of Physics and Electronic Information Technology, Yunnan Normal University, Kunming, China*

Oxygen vacancy has been suggested to play a role in the electrochemical ability of $NiMoO_4$. The band structure and density of state of $NiMoO_4$ bulks with different concentrations of oxygen vacancy were investigated by the first-principles calculation. Original $NiMoO_4$ shows semiconductive properties with a direct band gap of 0.136 eV. When one to three oxygen vacancies were introduced in the $NiMoO_4$ supercell, the band structure of $NiMoO_4$ transforms to metallic properties, and oxygen vacancies formation energy increases with the increased number of oxygen vacancies. The oxygen vacancies in $NiMoO_4$ lead to the increased electron localization of Ni 3d and Mo 3d state nearby the Fermi level, resulting in higher concentration of carriers in $NiMoO_4$ and thus increase in its electrical conductivity. The results demonstrate that introducing oxygen vacancies can improve the conductive property of $NiMoO_4$.

Keywords: density function theory, oxygen vacancies, formation energy, electronic structure, density of states (DOS)

OPEN ACCESS

Edited by:
Chao Han,
University of Technology Sydney, Australia

Reviewed by:
Junling Guo,
Zhengzhou University, China
Chong Wang,
Wuhan University of Science and Technology, China

***Correspondence:**
Chen Qing
qingchen1@126.com

Specialty section:
This article was submitted to Electrochemical Energy Conversion and Storage, a section of the journal Frontiers in Energy Research

Received: *11 October 2021*
Accepted: *21 October 2021*
Published: *18 November 2021*

Citation:
Wen Y, Wang P, Ding X, Feng X and Qing C (2021) Roles of Oxygen Vacancies in $NiMoO_4$: A First-Principles Study. Front. Energy Res. 9:793032. doi: 10.3389/fenrg.2021.793032

INTRODUCTION

As a typical transition metal oxides semiconductor, $NiMoO_4$ has attracted attention for its wide applications in electrochemical energy storage and conversion, such as supercapacitor and electrocatalytic water splitting (Du et al., 2018; An et al., 2019). However, the poor conductivity and electrochemical activity of $NiMoO_4$ limited its electrochemical energy storage performance. Defects engineering is a common method to change the physical chemistry property of transition oxide materials. As a typical representative of defects, oxygen vacancies can effectively modulate their electronic properties, tune their bandgaps, and optimize their electrical conductivity (Zhang et al., 2020a). It has been proven experimentally that oxygen vacancies also can alter the interlayer spacing of metal oxide to promote faster charge storage kinetics (Kim et al., 2017; Qing et al., 2018). However, theoretical mechanism analysis of oxygen vacancies in $NiMoO_4$ on its capacitance performance is still scarce.

$NiMoO_4$ has a typical monoclinic crystal structure. Both the Ni and Mo atoms are in octahedral site, and the distance between Mo and O atom was 2.3–2.4 Å (Rodriguez et al., 1998; Rodriguez et al., 2000). When redox reaction occurs, the Ni^{2+} has oxidized to Ni^{3+}; meanwhile, the MoO_4^{2-} framework remains stable. Due to the band gap of $NiMoO_4$ of 2.23 eV in natural temperature, the actual pseudo-capacitance performance of $NiMoO_4$ was unsatisfactory (Yang et al., 2016).

In order to understand the physical property of oxygen vacancies in $NiMoO_4$, we performed first-principles calculation on the electronic structure, total density of states (TDOS), and partial density of states (PDOS) of $NiMoO_{4-x}$ for the case of x = 0.0, 0.125, 0.250, and 0.375 (call NMO-0, NMO-1, NMO-2, NMO-3, respectively) by the Vienna Ab-Initio Simulation Package (VSAP) based on density functional theory (DFT). We have constructed a supercell of eight unit cells consisting of 48 atoms. Furthermore, in order to understand the relationship between vacancies structures and electrical properties in $NiMoO_4$, the formation energy of neutral oxygen vacancy in different chemical environments has been calculated.

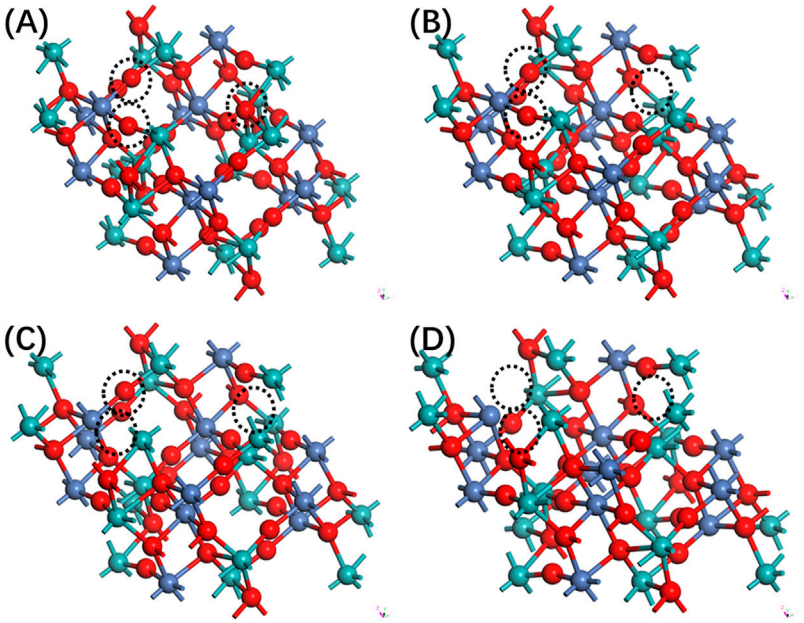

FIGURE 1 | The side view of configuration of $NiMoO_4$ with different oxygen vacancies. **(A)** Zero, **(B)** one, **(C)** two, and **(D)** three.

THEORETICAL MODEL AND COMPUTATIONAL METHOD

Theoretical Model

The study of oxygen vacancies in $NiMoO_4$ has been investigated by constructing a perfect supercell approach. Based on the optimized construction of perfect $NiMoO_4$, the unit cell is built by 2 × 2 × 2 in the *x*, *y*, and *z* directions, and a supercell consisting of 48 atoms is used for vacancies calculation. To introduce oxygen vacancies, an interior atom is removed from the supercell. The theoretical model is shown in **Figure 1**.

Computational Method

In order to understand the relationship between vacancies structures and electrical properties in $NiMoO_4$, the formation energy of neutral oxygen vacancy in different chemical environments was calculated. The corrected formation energy of an isolated neutral O vacancy in $NiMoO_4$ (ΔE_{Vo}) is defined as:

$$E_{V_0} = E_{defective} - E_{perfect} + \frac{1}{2}E_{O_2}$$

where $E_{defective}$ is the total energy of a structure with oxygen vacancies, $E_{perfect}$ is the total energy of the structure without oxygen vacancy, and E_{O2} is the elemental chemical potential of oxygen in the gas phase.

The DFT calculation was implemented in the Vienna Ab-Initio Simulation Package (Kresse and Joubert, 1999). For the exchange and correlation functionals, the Perdew–Burke–Ernzerhof (PBE) version of the generalized gradient approximation (GGA) exchange correlation was used (Blöchl, 1994; Perdew et al., 1996). In the DFT calculation, the $NiMoO_4$ bulks with different concentrations of oxygen vacancies were used to uncover the electronic properties. Vacuum layer thickness of 20 Å was applied to avoid virtual interaction and obtain more accurate results. The k-grid mesh value was 5 × 5 × 1. In addition, DFT + U method was also introduced to describe the electronic properties and vacancies states in $NiMoO_4$ bulks. The value of U given to Ni ions was 4 eV (Hinuma et al., 2007). The energy cutoff of 450 eV was used for the wave functions expansion. The energy and force converged to 1.0×10^{-5} eV $atom^{-1}$ and 0.03 eV $Å^{-1}$ to achieve high accuracy.

TABLE 1 | The formation energy of different concentrations of oxygen vacancy Vo in perfect $NiMoO_4$.

	$E_{(NMO)}$ (eV)	$E_{(NMO\_Vo)}$ (eV)	$E_{(O2)}$ (eV)	$\Delta E_{(form.\ energy)}$ (eV)
NMO-1	−355.63	−350.52	−8.75	0.73
NMO-2	−355.63	−344.92	−8.75	1.95
NMO-3	−355.63	−338.94	−8.75	3.56

RESULTS AND DISCUSSION

The calculated formation energy for different amount of oxygen vacancies in $NiMoO_4$ for a 2 × 2 × 2 bulk cell (48 molecular units) is shown in **Table 1**. The formation energy for different number of oxygen vacancies in $NiMoO_4$ was 0.73, 1.95, and 3.56 eV, respectively. The formation energy of two and three oxygen vacancies in $NiMoO_4$ are 2.67 and 4.88 times than that of the one vacancy, respectively, which suggested that one vacancy is more easily formed in $NiMoO_4$ crystal. This result shows that it is hard to synthesize two and three oxygen vacancies into $NiMoO_4$ under normal experimental conditions.

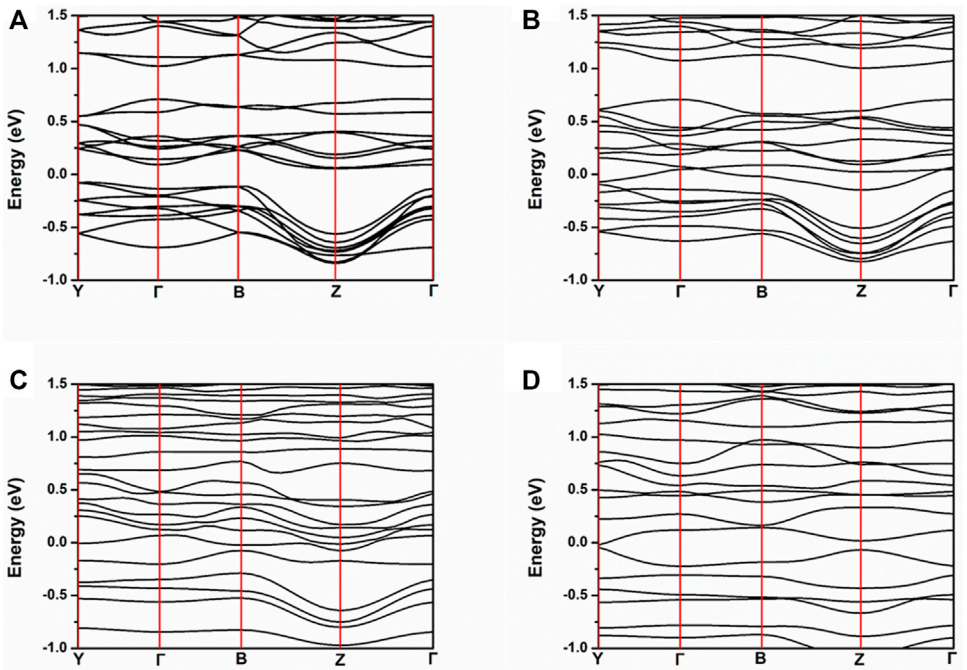

FIGURE 2 | Band structure of $NiMoO_4$ with different amounts of oxygen vacancies. **(A)** NMO-0, **(B)** NMO- 1, **(C)** NMO-2, and **(D)** NMO-3.

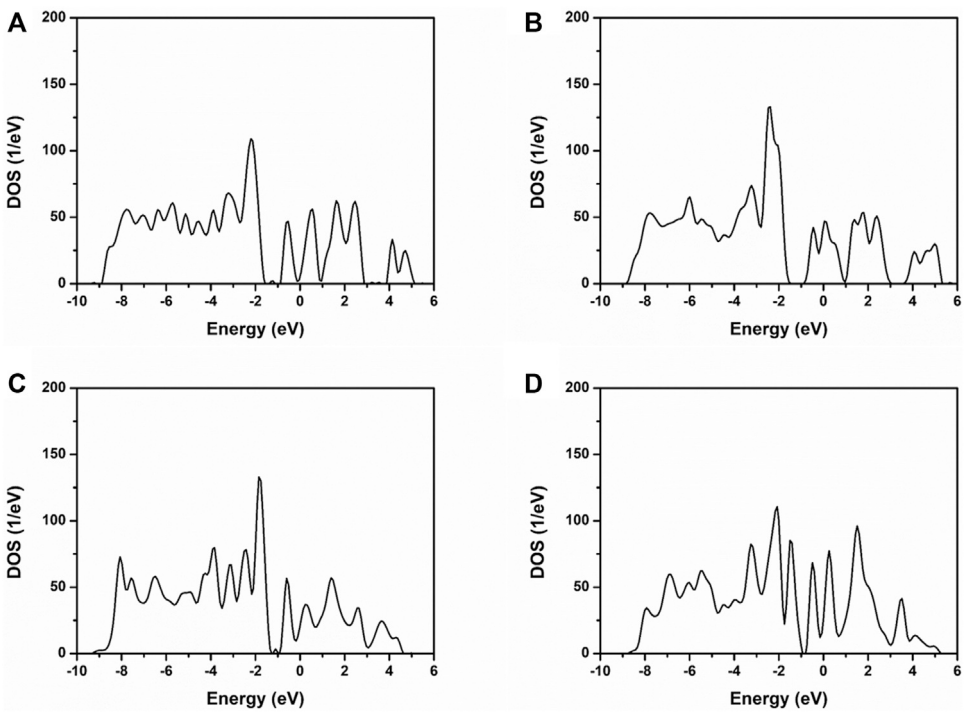

FIGURE 3 | TDOS of $NiMoO_4$ with different amounts of oxygen vacancies. **(A)** NMO-0, **(B)** NMO-1, **(C)** NMO-2, and **(D)** NMO-3.

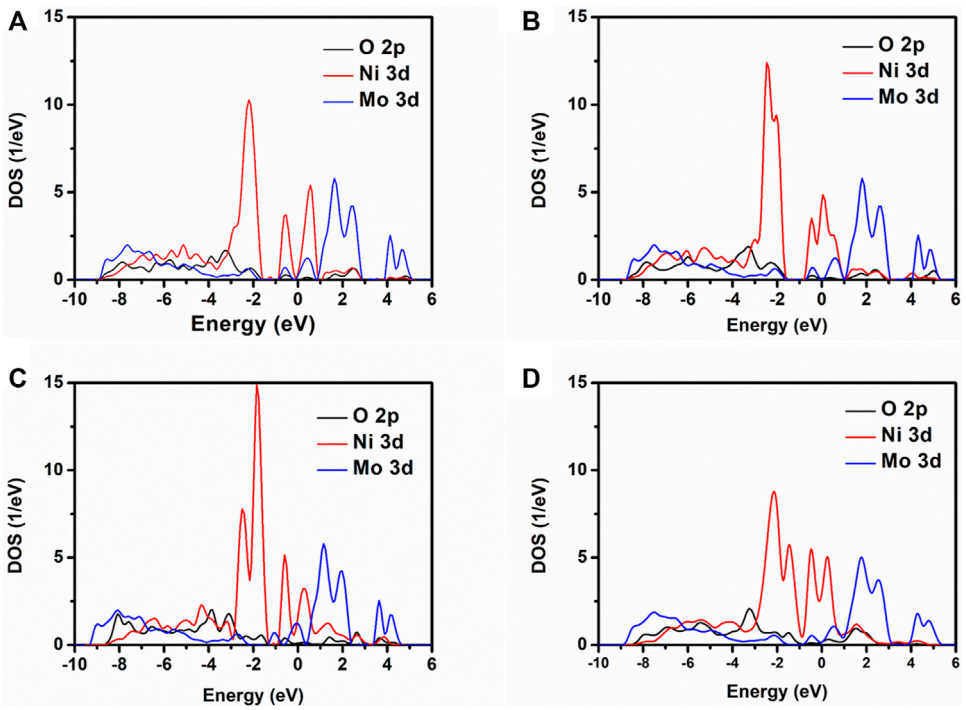

FIGURE 4 | PDOS for $NiMoO_4$ with different numbers of oxygen vacancies. **(A)** NMO-0, **(B)** NMO-1, **(C)** NMO-2, and **(D)** NMO-3.

In order to reveal the oxygen vacancy electron doping effect on the electronic structure of $NiMoO_4$, the band structure, TDOS, and PDOS, of stoichiometric $NiMoO_4$ in 2 × 2 × 2 supercell with different amount of oxygen vacancies were calculated. **Figure 2** shows the band structure of $NiMoO_4$ with different numbers of oxygen vacancies from zero to three. The Fermi levels of NMO-0, NMO-1, NMO-2, and NMO-3 were 6.1014, 6.0258, 5.9609, and 5.8729 eV, respectively. All of the Fermi levels were located at zero in all the figures. The valence band maximum of NMO-0 is located at −0.079 eV, and the conduction band minimum is located at 0.056 eV. NMO-0 is a semiconductor with an indirect gap of 0.136 eV. Furthermore, NMO-1, NMO-2, and NMO-3 showed metallic electrical conductivity characteristics. With the introduction oxygen vacancies into $NiMoO_4$, the extra-nuclear electrons of Mo have been released, which leading to increasing number of carrier concentration. The results are consistent with the DFT calculation result of SF Matar's work (Matar et al., 2010).

It can be obtained that the valence band of $NiMoO_4$ can be divided into lower and upper valence bands. The lower band mainly consisted of the O 2d, Ni 3d, and Mo 3d, as shown in **Figure 3**. The upper valence band consisted of Ni 3d and Mo 3d. While oxygen vacancies were introduced into the $NiMoO_4$ crystal, the band gap of $NiMoO_4$ has narrowed. The introduction of oxygen vacancies in $NiMoO_4$ gives more distribution of state density nearby the Fermi energy level, which indicates that more metallic properties of $NiMoO_4$ (Zhang et al., 2020b).

The PDOS of O 2p, Ni 3d, and Mo 3d for NMO-0, NMO-1, NMO-2, and NMO-3 are displayed in **Figure 4**. Nearby the Fermi level, the electronic states of $NiMoO_4$ mainly consist of Ni 3d and Mo 3d. With the number of oxygen vacancies from zero to three, the half-peak width of Ni 3d and Mo 3d decreased and exhibited higher electron localization effect. This suggests that $NiMoO_4$ has transformed to metallic properties with oxygen vacancies created into the $NiMoO_4$ crystal, which is in accordance with the calculation consequence of band structure.

CONCLUSION

In summary, we analyzed the formation energy, band structure, DOS, and PDOS from zero to three oxygen vacancies in 2 × 2 × 2 $NiMoO_4$ supercell with density functional theory calculation. The result revealed that only one oxygen vacancy can easily form in $NiMoO_4$ crystal. The original $NiMoO_4$ shows direct band gap semiconductor characteristic. With the amount of oxygen vacancies increase from one to three, the band gap of $NiMoO_4$ become narrower and exhibit stronger metallic properties. The electron state nearby the Fermi level of $NiMoO_4$ are mainly determined by Ni 3d and Mo 3d. Oxygen vacancies into $NiMoO_4$ accelerate the electron localization effect of Ni 3d and Mo 3d around the Fermi level.

DATA AVAILABILITY STATEMENT

The raw data supporting the conclusions of this article will be made available by the authors, without undue reservation.

AUTHOR CONTRIBUTIONS

All authors listed have made a substantial, direct, and intellectual contribution to the work, and approved it for publication.

FUNDING

The authors acknowledge the financial support of the Young Science Foundation of Yunnan (Grant No. 2019FD113), National Natural Science Foundation of China (11764047) and Education Science Foundation of Yunnan (2020J0095).

ACKNOWLEDGMENTS

The authors thank the Yunnan Key Lab of Opto-Electronic Information Technology.

REFERENCES

An, L., Feng, J., Zhang, Y., Wang, R., Liu, H., Wang, G.-C., et al. (2019). Epitaxial Heterogeneous Interfaces on N-NiMoO4/NiS2 Nanowires/Nanosheets to Boost Hydrogen and Oxygen Production for Overall Water Splitting. *Adv. Funct. Mater.* 29 (1), 1805298. doi:10.1002/adfm.201805298

Blöchl, P. E. (1994). Projector Augmented-Wave Method. *Phys. Rev. B* 50 (24), 17953–17979. doi:10.1103/PhysRevB.50.17953

Du, X., Fu, J., and Zhang, X. (2018). NiCo 2 O 4 @NiMoO 4 Supported on Nickel Foam for Electrocatalytic Water Splitting. *ChemCatChem* 10 (23), 5533–5540. doi:10.1002/cctc.201801419

Hinuma, Y., Meng, Y. S., Kang, K., and Ceder, G. (2007). Phase Transitions in the LiNi0.5Mn0.5O2 System with Temperature. *Chem. Mater.* 19 (7), 1790–1800. doi:10.1021/cm062903i

Kim, H.-S., Cook, J. B., Lin, H., Ko, J. S., Tolbert, S. H., Ozolins, V., et al. (2017). Oxygen Vacancies Enhance Pseudocapacitive Charge Storage Properties of MoO3−x. *Nat. Mater* 16 (4), 454–460. doi:10.1038/nmat4810

Kresse, G., and Joubert, D. (1999). From Ultrasoft Pseudopotentials to the Projector Augmented-Wave Method. *Phys. Rev. B* 59 (3), 1758–1775. doi:10.1103/physrevb.59.1758

Matar, S. F., Largeteau, A., and Demazeau, G. (2010). AMoO4 (A = Mg, Ni) Molybdates: Phase Stabilities, Electronic Structures and Chemical Bonding Properties from First Principles. *Solid State. Sci.* 12 (10), 1779–1785. doi:10.1016/j.solidstatesciences.2010.07.030

Perdew, J. P., Burke, K., and Ernzerhof, M. (1996). Generalized Gradient Approximation Made Simple. *Phys. Rev. Lett.* 77 (18), 3865–3868. doi:10.1103/PhysRevLett.77.3865

Qing, C., Yang, C., Chen, M., Li, W., Wang, S., and Tang, Y. (2018). Design of Oxygen-Deficient NiMoO4 Nanoflake and Nanorod Arrays with Enhanced Supercapacitive Performance. *Chem. Eng. J.* 354, 182–190. doi:10.1016/j.cej.2018.08.005

Rodriguez, J. A., Chaturvedi, S., Hanson, J. C., Albornoz, A., and Brito, J. L. (1998). Electronic Properties and Phase Transformations in CoMoO4 and NiMoO4: XANES and Time-Resolved Synchrotron XRD Studies. *J. Phys. Chem. B* 102 (8), 1347–1355. doi:10.1021/jp972137q

Rodriguez, J. A., Hanson, J. C., Chaturvedi, S., Maiti, A., and Brito, J. L. (2000). Phase Transformations and Electronic Properties in Mixed-Metal Oxides: Experimental and Theoretical Studies on the Behavior of NiMoO4 and MgMoO4. *J. Chem. Phys.* 112 (2), 935–945. doi:10.1063/1.480619

Yang, L., Wang, J., Wan, Y., Li, Y., Xie, H., Cheng, H., et al. (2016). Structure and Effective Visible-Light-Driven Photocatalytic Activity of α-NiMoO4 for Degradation of Methylene Blue Dye. *J. Alloys Comp.* 664, 756–763. doi:10.1016/j.jallcom.2015.10.037

Zhang, X., Liu, X., Zeng, Y., Tong, Y., and Lu, X. (2020a). Oxygen Defects in Promoting the Electrochemical Performance of Metal Oxides for Supercapacitors: Recent Advances and Challenges. *Small Methods* 4 (6), 1900823. doi:10.1002/smtd.201900823

Zhang, X., Su, H., and Du, X. (2020b). A Nickel Molybdenum Oxide Nanoarray as an Efficient and Stable Electrocatalyst for Overall Water Splitting. *New J. Chem.* 44 (20), 8176–8182. doi:10.1039/D0NJ01232G

Conflict of Interest: The authors declare that the research was conducted in the absence of any commercial or financial relationships that could be construed as a potential conflict of interest.

Publisher's Note: All claims expressed in this article are solely those of the authors and do not necessarily represent those of their affiliated organizations, or those of the publisher, the editors, and the reviewers. Any product that may be evaluated in this article, or claim that may be made by its manufacturer, is not guaranteed or endorsed by the publisher.